Part A: English Edition

Journal of Textiles and Polymers

Vol. 9, No. 1, 41-50, 2021

ORIGINAL PAPER

Effect of Seam Stabilizing Tapes on the Recovery Properties of Sewn Fabrics

Shohreh Minapoor[1*], Afsaneh Valipouri[2], and Arefeh Salehi[2]

Received: 23 May 2020, accepted: 29 September 2020

***Abstract*- Maintaining and improving the garment quality are the important topics in the textile and apparel industry. The aim of this paper is to investigate the influence of some textile tapes on elastic properties as well as dynamic recovery of the seams and enhance the shape stability. Three samples were prepared, namely weft knitted sewn fabrics without any stabilizing tape, and weft knitted sewn fabrics stabilized with bias woven fabric, and with stretch ribbons. The results show that hysteresis area of the seam tensile curves decreased by increasing the loading cycles, and dynamic work recovery stabilized after the third cycle. The tensile stress of all sewn samples in the course direction is significantly less than the stress value in the wale direction. It is found that the seams stabilized with stretch ribbons have the highest dynamic work recovery (~40-70%). Also, when the seam position and the loading direction aligned, the dynamic work recovery of the stabilized samples increased. The recovery behavior of the stabilized sewn fabrics was also simulated by mechanical models consisting of spring and dashpot elements. The three-element model, consisting of the Maxwell body paralleled with a non-linear spring, properly estimated the force–strain curves of the stabilized sewn fabrics under cyclic loading.**

***Keywords*: seam stabilizing tape, tensile behavior, dynamic work recovery, knitted fabric, mechanical model**

I. INTRODUCTION

Garment seams are exposed to various kinds of loads and deformations during daily human activities. Seam performance strongly affects the garment quality. Strength and elastic behavior of seams are important quality factors of sewn clothes, depending on different technical parameters, such as the type of fabric, sewing thread as well as its linear density, stitch density, and etc. These two agents should not allow seam breakage upon normal stresses of garments [1-4].

Elastic sport clothes play a great role in optimizing the consumer performance by providing freedom body movement. Clearly, in the absence of body motions, many garments provide reasonable comfort. As soon as the physical movement is made, the level of comfort performance significantly changes. Therefore, the elastic work needs to be measured over the body movements [5]. Knitted fabrics are widely used in elastic sport clothes due to having easy-care properties and high elastic recovery [6]. However, the seams sewn in these clothes exhibit a lower level of dynamic recovery compared with the knitted fabrics. Thus, most of the applied forces and tension concentration are exerted upon them. Enhancement of seams properties is subsequently required to improve the elastic recovery of garments. The elastic recovery and the shape stability of garments are improved by increasing the dynamic work recovery of the seams. Whereas, many researches have been done on seam pucker and other defects from past to present [7-9], few studies have been reported to investigate the elastic performance and recovery behavior of the seams. Previous studies have examined some methods to improve the elastic performance of the seams, such as changing the stitch density [10,11], the type of stitches [12], the linear density of sewing threads [12], the type or structure of sewing threads (twist per meter) [13], the type of fabrics, the direction of seams [14], and sewing conditions [15].

S. Minapoor
Department of Textile Engineering, University of Neyshabur, Neyshabur, Iran.

A. Valipouri and A. Salehi
Department of Textile Engineering, Isfahan University of Technology, Isfahan, Iran.

Correspondence should be addressed to S. Minapoor
e-mail: minapoor@neyshabur.ac.ir

TABLE I
CHARACTERISTICS OF FABRICS AND RIBBONS

Textile substances	Material*	Fabric structure	Nominal yarn linear density (Nm)	Density (/cm)	Thickness (mm)
Knitted fabric	80% P, 20% C	Interlock	70	CPC: 10.4 WPC: 14.8	0.43
Woven ribbon	Warp: 90% P, 10% C Weft: P	Plain	Warp: 69 Weft: 79	Warp: 45 Weft: 27	0.21
Stretch ribbon	P/E	Braid	-	-	1.07
Sewing thread	P	-	33.3	-	-

*C=Cotton, P=Polyester, and E= Elastane

Webster *et al.* investigated the effects of repeated extension and recovery on the physical properties of the ISO-301 stitched seams. They emphasized that there was a critical need to explain the ageing and failure of the seams relative to the changes of their mechanical properties as a consequence of tensile cycling. They found that the types of fabric as well as thread are two important parameters determining the breaking load and the extension of seams under tensile cycling [16]. It has been reported that the seam location is usually the weakest part on a garment, where great loads are exerted. The influence of loading on the seams in time intervals was analyzed by Rogina-Car and her colleagues. They found that the samples with seams had an approximately lower breaking force, equal to 70%, in comparison with the samples without seams [17]. On the other hand, when the garment is utilized, seam slippage might occur, leading to fabric opening at the seam line [18,19]. Kordoghli *et al.* investigated the load-elongation behavior of the seams and stated that it was more useful to study the yield point compared with the rupture point. According to the authors, in comparison with the plastic phase, the elastic phase (recovery) of a wear was more important, and the yield point of the seam could better illustrate the limit of the use of sewn fabrics. They reported that increasing the number of stitches per centimeter improved the breaking resistance of the seams, while the elongation-at-break did not change [20].

The advancement of high-quality garments requires an examination of novel techniques to increase the seam performance. The effect of the thermoplastic reinforcing tapes on the seam efficiency has just been investigated by Golomeova *et al.* [21]. It was found that the seam efficiency is generally increased with insertion a thermoplastic stitched reinforced tape in the seam structure.

Nowadays, improving the garment quality is an important topic in textile and apparel industry. Investigating the effectiveness of the reinforced and stabilizing tapes on seam efficiency as a novel technique would be valuable. Besides, the recovery after the load removal is a time-dependent process in the cyclic loading of the sewn fabrics, and the tensile properties of the sewn fabrics can subsequently be explained by the viscoelastic models [16,22,23]. However, the effect of stabilizing the seams, using elastic, and non-elastic textile materials on the mechanical performance of the garments has not yet been fully understood. The present work aimed to study the effect of the stabilized tapes, including bias woven fabric and stretch ribbons embedded in seams, on the tensile recovery and shape stability of the sewn fabrics. Also, a mechanical model was developed to explain the recovery behavior of the sewn fabrics after the

(a) (b) (c)

Fig. 1. Weft-knitted samples sewn with three different textile materials: (a) common sewing thread, (b) bias woven ribbon, and (c) stretch ribbon.

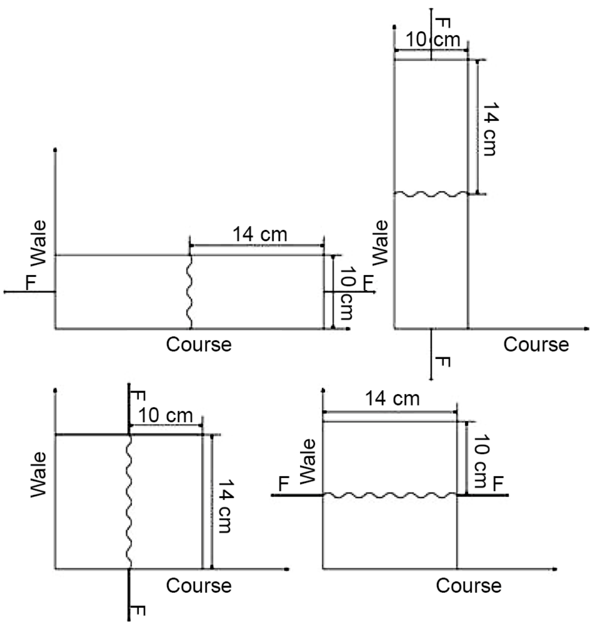

Fig. 2. Position of the seam (wavy lines) and loading direction.

tensile cyclic loading.

II. EXPERIMENTAL

A. Materials

A wide range of woven, knitted, and nonwoven fabrics is available for sport wears. Knitted fabrics are preferred due to greater elasticity and stretch ability [24]. Weft-knitted cotton/polyester fabrics, as the usual fabrics in the sport wears, were chosen for the tests. In order to investigate the tensile and dynamic elastic behavior of the stabilized seams, three different materials were used. Weft-knitted sewn samples without any seam stabilizing tape (sewn with a usual thread) and the sewn samples stabilized with bias woven fabrics and with stretch ribbons were prepared. Detailed information about the knitted fabrics and the used ribbons and thread is given in Table I.

As seams have different positions in garments and are subjected to loads in various directions, several conditions must be studied. To prepare the samples, the weft-knitted fabrics were cut into 14×10 cm^2 strips in both course and wale directions. The seams were sewn in both directions using three different textile materials: common sewing threads, bias woven ribbons, and stretch ribbons, as shown in Fig. 1. Therefore, using various sewing materials, positions of seams and two loading directions, namely course and wale directions, 12 different samples were prepared. All the samples were sewn with 504 stitches, SPI of 10 and 1.2 cm seam allowance using a Jack industrial lockstitch sewing machine, China, at speed of 4000 stitches/min. The positions of the seam as well as the loading direction

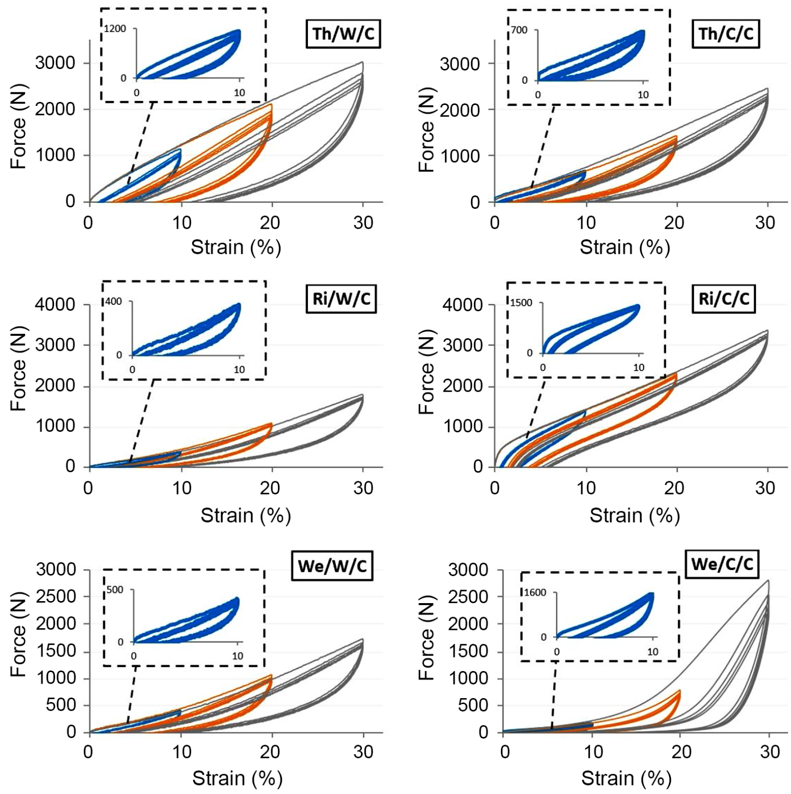

Fig. 3. Hysteresis of samples at 10, 20, and 30% extension levels, in course direction (shown by blue, orange, and grey lines, respectively).

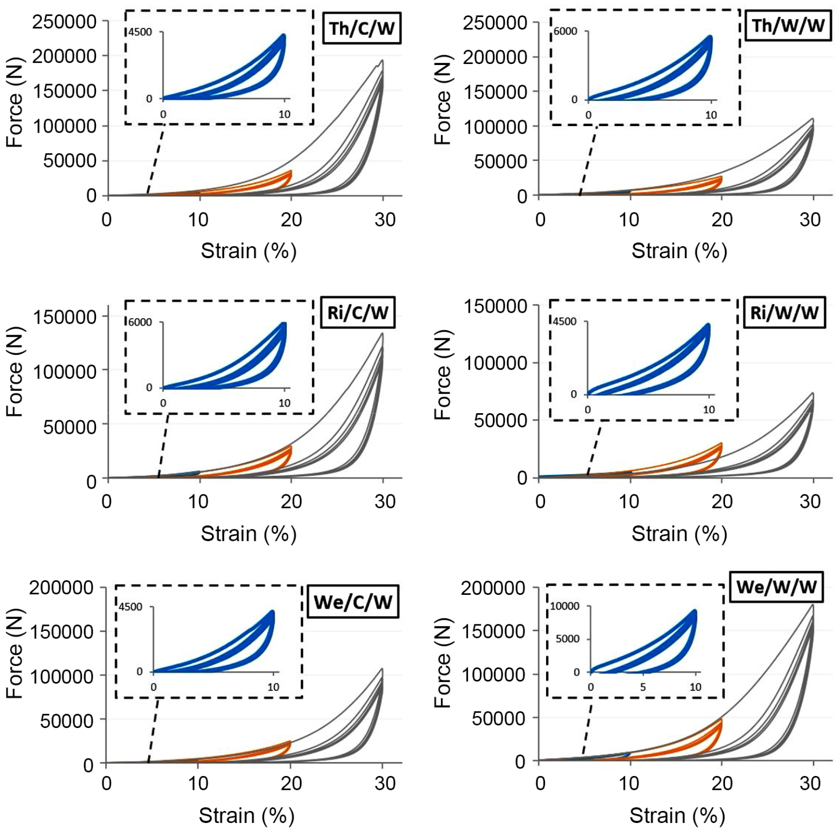

Fig. 4. Hysteresis of samples at 10, 20, and 30% extension levels, in wale direction (shown by blue, orange, and grey lines, respectively).

are shown in Fig. 2. It should be noted that fabrics were relaxed before and after sewing for 24 h on a flat surface (dry relaxation).

B. Tensile Test

Sewn samples were tested in terms of their dynamic elastic behavior according to ASTM D4964-96, standard test method for tension and elongation of elastic fabrics, in standard atmosphere for testing textiles, which is 21 °C (70 °F) and 65% relative humidity. The test was done at different extension levels, including 10, 20, and 30% extension, using a Zwick tensile tester (model 14460-Germany). These values were selected based on the human body movement [25]. The tension rate and the gauge length of the testing device were set to 100 mm/min and 10 mm, respectively. The cyclic tension test was performed in five cycles. Three specimens were prepared for each test, and eventually, the average force-strain curves were reported. Figs. 3 and 4 show the force-strain hysteresis of the samples under various levels of extension and different recovery processes. It should be noted that the samples coding was performed using the initial letters of the seam materials, the positions of the seam and the loading direction (The abbreviations used were as follows: Th for thread, Ri for stretch ribbon, We for weave, C for course direction, and W for wale direction).

C. Mechanical Model

Textile materials have both viscous and elastic properties. The viscous behavior is based on the Newtonian fluid, while the elastic trend is in accordance with the Hookean solid. Most of the textile materials conduct linearly elastic under lower levels of extension. An increase in the level of extension leads the response of the textile materials reaching the viscoelastic extension, which is recoverable using a definite-time component. At higher level of extension, the textile material has a non-linear viscoelastic behavior, and the extension grows more rapidly in comparison with the stress [22]. Mechanical models containing springs and viscose dashpots have frequently been employed to understand and explain the viscoelastic properties of the textile materials in numerous studies [26]. However, there have been few studies on the viscoelastic tensile behavior and recovery properties of the sewn garment. In this study, simple mechanical models were developed and validated to describe the behavior of the seams under constant rates

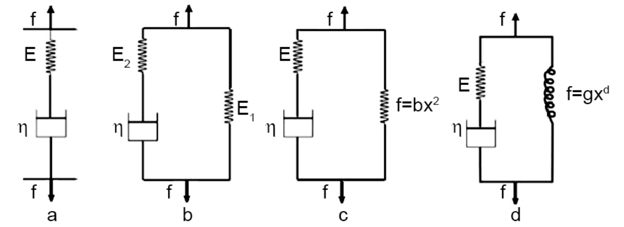

Fig. 5. Mechanical viscoelastic models: (a) Maxwell model, (b) standard linear model, (c) standard nonlinear model, and (d) Manich model.

of tension and recovery process. To do so, four different rheological models were designed. As seen in Fig. 5, in both Maxwell and standard linear models, the springs and dashpots obeyed the Hook's and Newton's laws, respectively. The nonlinear three-element model, known also as the Vangheluwe model, consisted of a Maxwell body connected in a parallel way with a nonlinear spring. The last structure was the Manich model having a nonlinear spring assumed to follow the power law, parallel to the Maxwell body [26,27].

The tensile test was performed at a constant rate (x=ct, wherein c was the test speed in m/s). Considering the boundary condition in which the applied force was zero in the initial time and substituting the differential equations governing the models, the force-displacement relationship in the tensile mode (f_t-x) could be derived for all four models as follows:

$$\text{Model (a)}: f_t = c\eta\left(1-e^{-\frac{E}{c\eta}x}\right) \tag{1}$$

$$\text{Model (b)}: f_t = E_1x + c\eta\left(1-e^{-\frac{E_2}{c\eta}x}\right) \tag{2}$$

$$\text{Model (c)}: f_t = bx^2 + c\eta\left(1-e^{-\frac{E}{c\eta}x}\right) \tag{3}$$

$$\text{Model (d)}: f_t = gx^d + c\eta\left(1-e^{-\frac{E}{c\eta}x^h}\right) \tag{4}$$

Where, f is the force in N, x is the displacement in m, E is the spring constant in N/m, η is the dashpot constant in N.s/m, and b, g, d, and h are constants.

The extension continued up to a certain point, i.e. x_1 (10, 20, and 30% extension). At this point, the tensile tester bounced back. The boundary condition for this mode was defined as follows: at the point x_1, the applied force was equal to f_1 (x_1 and f_1 were the coordinates of the last point under the tensile mode); as continued, the applied force reduced by the passage of time. Therefore, the force-displacement relationship in this mode (f_r-x for x<x_1) could be derived for all four models as follows:

$$\text{Model (a)}: f_r = (f_1 + c\eta)e^{-\frac{E}{c\eta}(x_1-x)} - c\eta \tag{5}$$

$$\text{Model (b)}: f_r = (f_1 + c\eta)e^{-\frac{E_2}{c\eta}(x_1-x)} - E_1(x_1-x) - c\eta \tag{6}$$

$$\text{Model (c)}: f_r = (f_1 + c\eta)e^{-\frac{E}{c\eta}(x_1-x)} - b(x_1-x)^2 - c\eta \tag{7}$$

$$\text{Model (d)}: f_r = (f_1 + c\eta)e^{-\frac{E}{c\eta}(x_1-x)^h} - g(x_1-x)^d - c\eta \tag{8}$$

The model parameters have been extracted using the non-linear optimization algorithm [26]. Using the experimental data obtained from the force-extension curves, several simulations were conducted based on the above equations, and the best model was developed to verify whether the force-extension curve of the sewn samples fitted the data.

III. RESULTS AND DISCUSSION

A. Experimental Results and Statistical Analysis

To study the dynamic tensile behavior of the sewn fabrics, the force-strain hysteresis of the samples was obtained and analyzed under different extension levels, in both course and wale directions. Figs. 6 and 7 show the tensile and recovery properties of the sewn samples together with the employed textile materials (knitted fabrics, woven ribbons and stretch ribbons). Here, the tensile stress and the dynamic work recovery (DWR) were set at 30% extension. It should be noted that the charts for other levels of extension are not provided here because they were all alike. The recovery behavior of a garment is important as it can enhance the body movement during intensive activities. In general, elastic textile materials result in minimum loss of energy, which can be calculated by measuring DWR [5]. DWR of a fabric is calculated using the following equation:

$$\text{Dynamic work recovery (\%)} = \left(\frac{\text{Area under the unloading curve}}{\text{Area under the loading curve}}\right)\times 100 \tag{9}$$

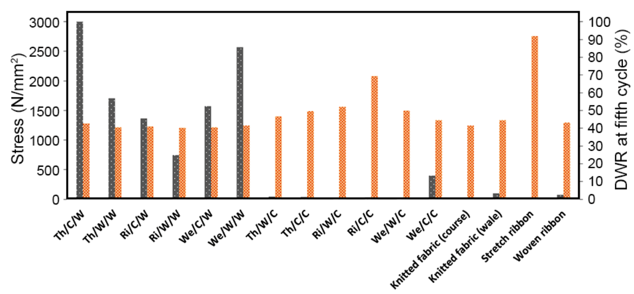

Fig. 6. Results of tensile and recovery properties of samples and materials at 30% extension.

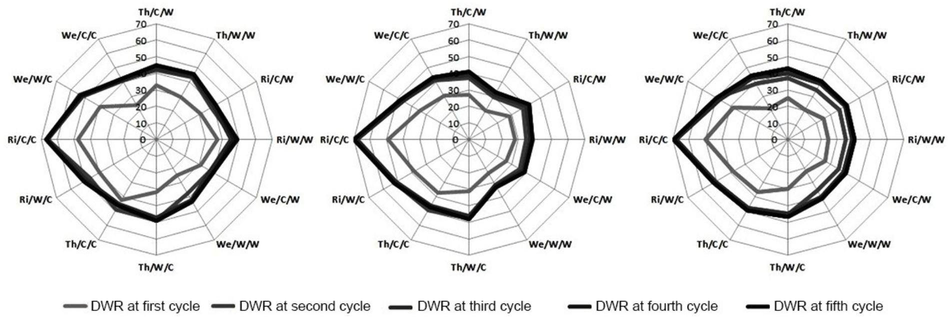

(a) (b) (c)

Fig. 7. Comparison of results of DWR in different cycles at: (a) 10% extension, (b) 20% extension, and (c) 30% extension.

As seen in Fig. 7, the tensile recovery behavior of the samples, at the first cycle of extension, was unrepeatable, and different from that of the other cycles. The hysteresis area of the tensile curves decreased by increasing the loading cycles, and the recovery properties were stabilized after the third cycle. Therefore, DWR of the samples increased due to reduction in the loading curve after the first cycle. According to the pervious literature, the area within the hysteresis loop measures energy dissipation in each cycle. In general, the difference between the hysteresis in the first cycle and the second cycle is the maximum. The energy required for stretching the fabric in the first cycle indicates the ability of fabric to resist tension at the initial stage. After that, the resistance of the fabric structure decreases because of moving yarns and changing the geometry of the loops to get closer to jamming. The difference among further cycles decreased as the number of cycles increased. If textile materials are repeatedly taken through a given cycle of stress, the loading and unloading curves in successive cycles will gradually get closer together until they form a continuous repeated loop [28,29].

According to Fig. 6, the tensile stress of all sewn samples in the course direction was significantly less than the stress value in the wale direction. When the tensile load was applied to the weft-knitted fabrics, the yarns frictionally moved and the geometry of the loops changed until jamming occurred. The wale-wise jamming took place sooner than the course-wise jamming due to the structure of the weft-knitted fabric and the form of the loop [30]. Hence, less force was needed at the same level of extension in the course direction, as seen in Figs. 3 and 4.

The results showed that the seams stabilized with stretch ribbons had the highest DWR. Obviously, the stretch ribbons had the highest DWR value (~90%) among the used textile materials. The DWR values of the seamless weft-knitted fabrics (in wale/course directions) and woven fabrics were also close to each other (~42%). The DWR of the seams stabilized with woven fabric was between these values, i.e. approximately 42 and 55%, by applying the tensile load in wale and course directions, respectively. The loop form in the weft-knitted structure resulted in more elasticity in the course direction which was intensified by stabilized stretch ribbons.

When the seam position and the loading direction aligned, the DWR of the stabilized samples increased. When the seam was horizontally extended, the tension was directly applied to the seam. Therefore, the stabilizing tapes embedded in the seams played an important role in the mechanical behavior of the seams. When the tensile load was vertically applied, the seam would be extended after the extension of the fabric structure. Therefore, the dynamic work recovery was affected by both the fabrics and the seams. According to the results, the damping energy of the seams stabilized with stretch ribbons was the least among all the seams. As expected, Ri/C/C and Ri/W/C had the highest DWR values and the least tensile stress, respectively (~70% and ~53%). Taguchi analysis also confirmed the results, as seen in Fig. 8. The direction of loading had the greatest effect on the DWR values. The type of stabilizing tapes embedded in the seams was

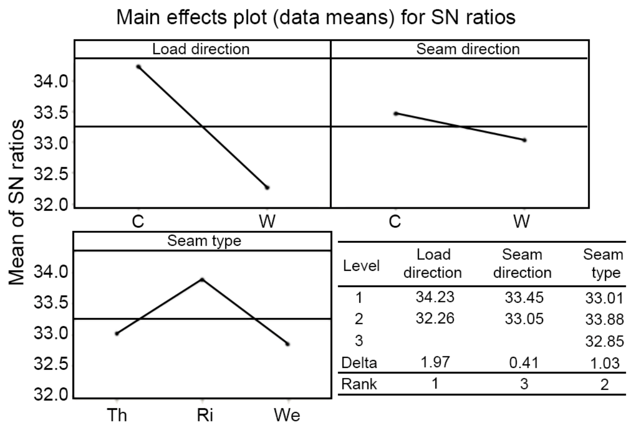

Level	Load direction	Seam direction	Seam type
1	34.23	33.45	33.01
2	32.26	33.05	33.88
3			32.85
Delta	1.97	0.41	1.03
Rank	1	3	2

Fig. 8. Main effects plot for SN ratios and response table for DWR.

second, followed by the seam position. However, only load direction has a statistically significant effect on DWR based on SPSS 16.0 statistical analysis.

B. Comparing the Mechanical Models

In this study, four viscoelastic models were developed to describe the tensile mechanical behavior of the sewn fabrics. It was incumbent to fit the experimental data with the models equations using the least square method so as to derive the parameters of the viscoelastic models. The viscoelastic models for predicting the tensile properties and recovery performance of the sewn fabrics were provided and their results were analyzed. Due to the similarity of the tensile behavior in all cycles (the form of tensile diagram), just one tensile cycle was applied. Fig. 9 shows the performance of the studied models employed to estimate the tensile mechanical behavior of the sewn fabrics in both directions (related to Ri/W/C and Ri/C/W samples). It must be noted that the curves as well as the extension levels of other samples followed a similar trend; they are not presented here due to space constraints.

It can clearly be observed in Fig. 9 that the linear models were not useful for demonstrating the non-linear behavior of the sewn structures, especially in tensile mode of hysteresis. When the force is applied in the course direction, the fitted curve of the standard non-linear model was closely in line with the experimental data in both tensile and recovery modes. However, in the wale direction, the model did not well match the data. As previously stated, the tensile force of all sewn samples in the wale direction was significantly higher than the force value in the course direction, and the major increase in the force occurred at the end of extension. The force-strain curves for both wale and course directions demonstrate highly non-linear behavior. Each curve can be divided into two generic zones: the first zone with low elasticity modulus and the second zone with high elastic modulus. The first zone occurs when the yarn moves within the structure with friction deforming

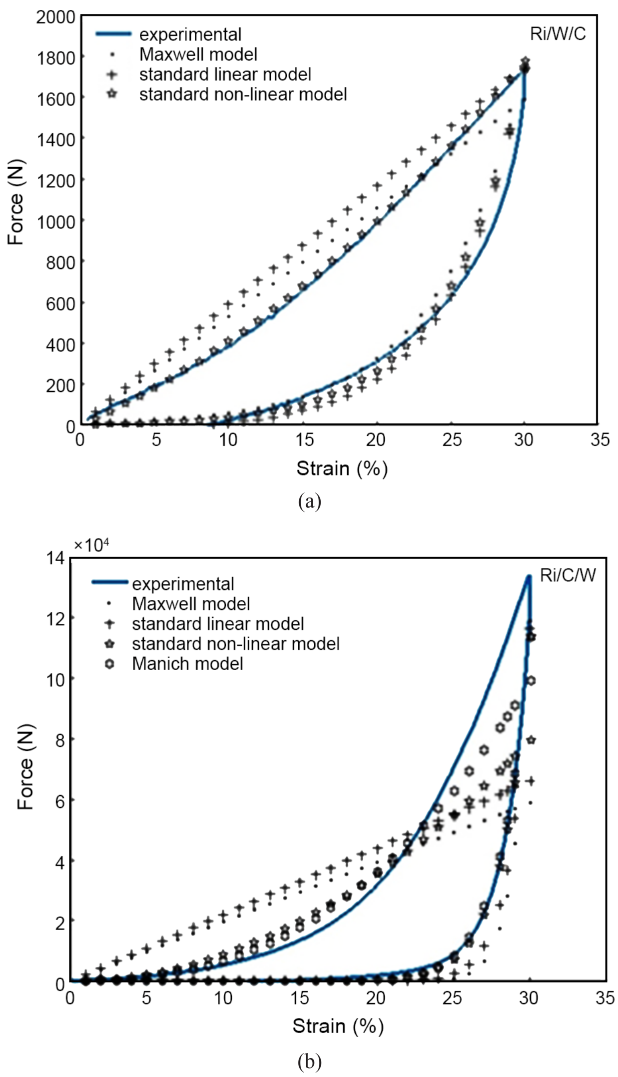

Fig. 9. Typical comparison between performances of different mechanical models to describe mechanical behavior and recovery processes of sewn fabrics: (a) Ri/W/C sample in course direction and (b) Ri/C/W sample in wale direction.

the loops. The second zone corresponds to the situation when each yarn elongates until it breaks [30]. The plain

TABLE II

PERFORMANCE OF DIFFERENT MECHANICAL MODELS TO FIT THE HYSTERESIS IN THE COURSE DIRECTION

Sample code	R-square		
	Maxwell	Standard linear	Standard non-linear
Th/W/C	0.95	0.92	0.97
Th/C/C	0.96	0.94	0.98
Ri/W/C	0.96	0.94	0.99
Ri/C/C	0.94	0.91	0.97
We/W/C	0.96	0.94	0.98
We/C/C	0.92	0.89	0.96

TABLE III
PERFORMANCE OF DIFFERENT MECHANICAL MODELS TO FIT THE HYSTERESIS IN THE WALE DIRECTION

Sample code	R-square			
	Maxwell	Standard linear	Standard non-linear	Manich
Th/C/W	0.68	0.67	0.86	0.92
Th/W/W	0.71	0.71	0.88	0.94
Ri/C/W	0.70	0.69	0.87	0.93
Ri/W/W	0.72	0.71	0.89	0.95
We/C/W	0.71	0.71	0.90	0.94
We/W/W	0.70	0.69	0.87	0.92

TABLE IV
MECHANICAL PARAMETERS OF MODELS

Sample code	E ($N/m\times10^3$)	η ($N.s/m\times10^3$)	b	g	d	h
Th/W/C	1247.3	1128.3	9.07	-	-	-
Th/C/C	621.3	873.8	10.42	-	-	-
Ri/W/C	2321.1	774.5	12.46	-	-	-
Ri/C/C	2553.7	660.1	18.71	-	-	-
We/W/C	248.3	526.5	10.06	-	-	-
We/C/C	536.8	800.4	8.17	-	-	-
Th/C/W	3741.4	2.29×10^{15}	-	23.68	3.71	2.67
Th/W/W	4224.6	5.42×10^{15}	-	138.68	2.92	1.05
Ri/C/W	5528.7	0.91×10^{15}	-	184.14	3.21	0.96
Ri/W/W	3443.5	6.31×10^{15}	-	87.86	3.43	1.02
We/C/W	3087.1	2.38×10^{15}	-	26.91	4.05	1.28
We/W/W	2573.2	1.29×10^{15}	-	43.69	3.46	0.94

TABLE V
EXPERIMENTAL AND PREDICTED VALUES OF THE SWEN FABRIC PROPERTIES

Sample code	DWR (%)		Initial tensile modulus ($N/m\times10^3$)	
	Experiment	Model	Experiment	Model
Th/W/C	46.8	42.1	0.93	0.94
Th/C/C	49.5	48.9	0.52	0.57
Ri/W/C	52.1	52.6	0.21	0.24
Ri/C/C	69.4	60.2	4.06	3.16
We/W/C	49.9	48.2	0.27	0.28
We/C/C	44.6	45.3	1.49	1.56
Th/C/W	42.7	43.2	7.13	7.22
Th/W/W	40.5	39.67	5.42	5.51
Ri/C/W	41.1	42.6	5.32	5.54
Ri/W/W	40.2	41.3	2.72	2.79
We/C/W	40.4	39.5	4.59	4.67
We/W/W	41.4	42.9	6.81	6.94

weft knitted fabric has less elongation in the wale-wise direction than in the course-wise due to the structure and form of the loops. Therefore, a great increase in the force occurred at the end of the cycle. In the other words, the low elasticity modulus region was followed by a rapid increase in the tensile force at the second zone. According to this a greater power function was needed for modelling in the wale direction. The Manich model with a nonlinear spring which was assumed to follow the power law better matched the data in this case. The fitting performances of four rheological models are presented in Tables II and III. In the recovery mode, the force-displacement curve followed a hysteresis path and showed residual deformation at zero force. The Zwick tensile tester automatically stopped at the intended extension and bounced back. Hence, the stretch sewn fabrics could start the recovery mode. It can be seen that all models were approximately capable of explaining the recovery behavior of the sewn fabrics after the removal of the load.

Having the equations governing the models and the experimental data, the mechanical parameters of the models were easily appraised. Table IV shows the estimated values of the models. As can be seen, when the tensile force was applied in the course direction, the values of the spring constants in Ri/C/C and Ri/W/C samples were higher than those of other samples. The seams stabilized with the stretch ribbons showed greater elasticity, while other seams exhibited higher viscosity. When the tensile force was applied in the wale direction, the seam behavior followed the Manich model, and the dashpot constants were higher than the spring constants in all samples. A low modulus region can evidently be seen in Fig. 4, followed by a rapid increase in the tensile force at the final values of extension. Finally, the comparison between the experimental and predicted values is illustrated in Table V. As can be seen, the predicted values obtained from the models are acceptably close to the experimental values.

IV. CONCLUSION

It is of great importance to enhance the tensile and elastic properties of the seams in order to achieve greater garment comfort, elastic recovery, and shape stability. The elastic recovery of the garment was improved by increasing the dynamic work recovery of the seams. This study investigated the influence of the stabilizing tapes as a novel technique on seam efficiency. The results showed that using stabilizing tapes, such as woven fabrics or stretch ribbons, the seam enhanced the tensile behavior and recovery properties of the garment. The tensile stress values of all sewn samples in the course direction were significantly less than the stress values in the wale direction due to the structure of weft-knitted fabrics and the form of the loops. The seams stabilized with the stretch ribbons had the highest DWR values, equal to 52 and 70%, in the wale and course directions, respectively. Taguchi analysis confirmed the experimental results and showed the effect of the seam stabilizing on DWR values. The results also showed that the three-element model, consisting of a Maxwell body parallel to a non-linear spring, could describe the tensile and recovery behavior of the sewn fabrics more accurately in comparison with the Maxwell and standard linear models. The standard non-linear and Manich models were appropriate for the tensile behavior in the course and wale directions, respectively. The assessment and modelling of the tensile and recovery behavior of the sewn garments under the applied levels of the extension are necessary to study the energy losses or the power gains, especially for people having high levels of activities.

REFRENCES

[1] D. Barbulov–Popov, N. Cirkovic, and J. Stepanović, “The influence of stitch density and of the type of sewing thread on seam strength”, *Tem J.*, vol. 1, no. 2, pp. 104-110, 2012.

[2] Z. Yildiz, V. Dal, M. Ünal, and K. Yildiz, “Use of artificial neural networks for modeling of seam strength and elongation at break”, *Fibres Text. East. Eur.*, vol. 5, no. 101, pp. 117-123, 2013.

[3] I. Frydrych and A. Greszta, “Analysis of lockstitch seam strength and its efficiency”, *Int. J. Cloth. Sci. Tech.*, vol. 28, no. 4, pp. 480-491, 2016.

[4] D. Vijay Kirubakar Raj and M. Renuka Devi, “Performance analysis of the mechanical behaviour of seams with various sewing parameters for nylon canopy fabrics”, *Int. J. Cloth. Sci. Tech.*, vol. 29, no. 4, pp. 470-482, 2017.

[5] S. Mani and N. Anbumani, “Dynamic elastic behaviour of cotton and cotton/spandex knitted fabrics”, *J. Eng. Fibers Fabr.*, vol. 9, no. 1, pp. 93-100, 2014.

[6] A. Mansor, S.A. Ghani, and M.F. Yahya, “Knitted fabric parameters in relation to comfort properties”, *Am. J. Mater. Sci.*, vol. 6, no. 6, pp. 147-151, 2016.

[7] R.M. Crow and M.M. Dewar, “Stresses in clothing as related to seam strength”, *Text. Res. J.*, vol. 56, no. 8, pp. 467-473, 1986.

[8] C.M.C. Dorkin and N.H. Chamberlain, *Seam Pucker: Its Cause and Prevention,* Clothing Institute, 1961, pp. 2-21.

[9] M. Shiloh, “The evaluation of seam-puckering”, *J. Text. I.*, vol. 62, no. 3, pp. 176-180, 1971.

[10] K. Phebe Aaron and B. Chandrasekaran, “Studies on influence of stitch density and stitch type on seam

properties of garment leathers", *AATCC J. Res.*, vol. 1, no. 6, pp. 8-15, 2014.

[11] R. Namiranian, S. Shaikhzadeh Najar, S.M. Etrati, and A.M. Manich, "Seam slippage and seam strength behaviour of elastic woven fabrics under static loading", *Indian J. Fibre Text. Res.*, vol. 39, no. 3, pp. 221-229, 2014.

[12] S. Malek, B. Jaouachi, F. Khedher, S. Ben Said, and M. Cheikhrouhou, "Influence of some sewing parameters upon the sewing efficiency of denim fabrics", *J. Text. I.*, vol. 108, no. 12, pp. 2073-2085, 2017.

[13] I. Ajiki and R. Postle, "Viscoelastic properties of threads before and after sewing", *Int. J. Cloth. Sci. Tech.*, vol. 15, no. 1, pp. 16-27, 2003.

[14] G. Busiliene, E. Strazdiene, V. Urbelis, and S. Krauledas, "The investigation of knitted materials bonded seams behaviour upon cyclical fatigue loading", *Mater. Sci.*, vol. 23, no. 2, pp. 180-185, 2017.

[15] A.K. Choudhary and A. Goel, "Effect of some fabric and sewing conditions on apparel seam characteristics", *J. Text.*, vol. 4, 2013. Available: http://dx.doi.org/10.1155/2013/157034

[16] J. Webster, R.M. Laing, and B.E. Niven, "Effects of repeated extension and recovery on selected physical properties of ISO-301 stitched seams: part I: load at maximum extension and at break", *Text. Res. J.*, vol. 68, no. 11, pp. 854-864, 1998.

[17] B. Rogina-Car, I. Schwarz, and S. Kovačević, "Analysis of woven fabric at the place of the sewn seam", *Autex Res. J.*, vol. 18, no. 3, pp. 216-220, 2018.

[18] K. Yildirim, "Predicting seam opening behaviour of woven seat fabrics", *Text. Res. J.*, vol. 80, no. 56, pp. 472-480, 2010.

[19] A. Gurarda and B. Meric, "Slippage and grinning behaviour of lockstitch seams in elastic fabrics under cyclic loading conditions", *J. Text. Appar. Tekst. Konfeks.*, vol. 20, no. 1, pp. 65-69, 2010.

[20] B. Kordoghli, M. Cheikhrouhou, and C.K. Saidene, "Mechanical behaviour of seams on treated fabrics", *Autex Res. J.*, vol. 9, no. 3, pp. 87-92, 2009.

[21] S. Golomeova and G. Demboski, "The influence of the thermoplastic reinforcement tape location on the seam performance", *Adv. Technol.*, vol. 6, no. 1, pp. 93-95, 2017.

[22] D.Š. Gorjanc and V. Bukosek, "The behaviour of fabric with elastane yarn during stretching", *Fibres Text. East. Eur.*, vol. 16, no. 3, pp. 63-68, 2008.

[23] R.J. Bassett, R. Postle, and N. Pan, "Experimental methods for measuring fabric mechanical properties: a review and analysis", *Text. Res. J.*, vol. 69, no. 11, pp. 866-875, 1999.

[24] D. Uttam, "Active sportswear fabrics", *Int. J. It. Eng. Appl. Sci. Res.*, vol. 2, no. 1, pp. 34-40, 2013.

[25] J. Voyce, P. Dafniotis, and S. Towlson, "Elastic textiles", in *Textiles in Sport*, Woodhead, 2005, pp. 204-230.

[26] S. Khavari and M. Ghane, "An analytical approach for the compression and recovery behaviour of cut pile carpets under constant rate of compression by mechanical models", *Fibers Polym.*, vol. 18, no. 1, pp. 190-195, 2017.

[27] A. Serwatka, P. Bruniaux, and I. Frydrych, "New approach to modelling the stress-strain curve of linear textile products part 1-theoretical considerations", *Fibres Text. East. Eur.*, vol. 14, no. 1, pp. 30-35, 2006.

[28] J.W. Hearle and W.E. Morton, *Physical Properties of Textile Fibres*, Elsevier, 2008, pp. 346-347.

[29] F.K. Ko and L.Y. Wan, "Engineering Properties of Spider Silk". in *Handbook of Properties of Textile and Technical Fibres*, 2nd ed., A.R. Bunsell Ed. Woodhead, 2018, pp. 195-200.

[30] O. Kononova, A. Krasnikovs, K. Dzelzitis, G. Kharkova, A. Vagel, and M. Eiduksa, "Modelling and experimental verification of mechanical properties of cotton knitted fabric composites/Silmuskootud puuvillakangast komposiitide mehaaniliste omaduste modelleerimine ja vordlemine katsetulemustega", *Est. J. Eng.*, vol. 17, no. 1, pp. 39-51, 2011.